A Review on the Drag Reduction Methods of the Ship Hulls for Improving the Hydrodynamic Performance

Mohammad Ahmadzadehtalatapeh[1*], Majid Mousavi[2]

[1]*Department of Marine & Mechanical Engineering, Chabahar Maritime University, Chabahar, Iran; m_ahmadzadeh56@yahoo.com*
[2]*Department of Naval Architecture Engineering, Chabahar Maritime University, Chabahar, Iran; s.majid.mousavi88@gmail.com*

ARTICLE INFO	ABSTRACT
	Hydrodynamic performance of a marine vessel mainly depends on the frictional and pressure resistance. Pressure drag reduction could be achieved by improving the shape of the vessels with implementation of modern hull forms. Hull forms optimization techniques could also be used for this purpose. Other techniques are needed to deal with the viscous portion of the total resistance, which is mainly frictional resistance. In this paper, an extensive literature review on the different methods applied to reduce the resistance of marine vessels was made, and the advantages and disadvantages of the implemented methods were identified. The related papers were categorized into three main categories and a summary of experimental and theoretical studies was provided. On the basis of results obtained from the reviewed research studies, the combination of hull form optimization methods with other applicable drag reduction technologies such as antifouling coating is recommended to optimize the hydrodynamic forces.

1. Introduction

The quest to achieve higher speeds together with low fuel consumption in marine transportation has been always one of the main objectives of naval architects. Marine industries transport 95% of the world's cargo and up to 85% of the available energy in ships is applied to overcome hydrodynamic forces [1,2]. Hull resistance is considered as the paramount importance to the ships or marine vessels, and it directly affects the speed, power requirements and fuel consumption.

Several techniques are exists to achieve drag reduction on marine vehicles. The main objective of these techniques is to find efficient ways to reduce the total resistance. Hydrodynamic performance of a ship could be improved by decreasing the frictional and pressure resistance.

Pressure drag reduction could be achieved by the improving the shape of the vessel by application of modern hull forms or hull forms optimization techniques.

In general, optimization methods focuses on minimizing the resistance by mainly reducing the wave resistance. For high-speed ships, wave making resistance is one of the main parameters needs to be considered in the optimization process [3,4].

Furthermore, new hull forms have been successful in reducing the level of residuary drag and their applications in various fields, notably in military applications have been accepted. The importance of this matter has encouraged the researchers to design and build new types of marine vehicles with different physical features.

Other techniques are needed to deal with the viscous portion of the total resistance. Frictional drag is the dominant part of the overall resistance, particularly in the merchant ships sailing at low speeds. Therefore, its reduction through surface characteristics improvement methods such as: applying antifouling and coatings, air lubrication techniques, and the use of riblets is a major challenge for the ship designers. Implementation of these methods through the boundary layer control reduces the surface drag of the underwater vehicles by delaying the onset of turbulent flow in the boundary layer. Turbulent flows can occur in the boundary layer near solid surfaces and the associated friction increases, as the flow velocity increases. Turbulence friction can make considerable losses in energy [5].

This literature survey has been separated into three main sections, which focused in turn on the hull forms

and its optimization, air lubrication, and fouling and coatings. For every category, the related studies and reports have been reviewed and discussed in the sub sections.

2. Hull Form Optimization

Hull form optimization from a hydrodynamic performance point of view is an important aspect of preliminary ship design. Due to the complexity and dynamics of ship design, naval architects try to use different types of reliable and adaptive approaches to improve the design quality. In addition, hydrodynamic optimization of ship hull reduces manufacturing costs and increases maritime safety, and consequently decreases the amount of carbon dioxide emission in the environment. Moreover, ship building industries are focusing on developing new design concepts and technologies towards fuel economic ship designs.

The classical design process consists of three steps, namely geometric modeling, hydrodynamic analysis, and optimization technologies. Implementation of these processes requires a proper understanding and practical design experience.

For ships hydrodynamic optimization, all objective functions such as: resistance, stability, and seakeeping must be considered. Considering one of the objectives alone will make unrealistic and impractical results. For instance, Biliotti et al. (2011) and Gammon [6,7] considered two or three objective functions in their work, while one objective function was considered for hull form optimizing by Han et al. (2012) and Matulja and Dejhalla [8,9].

Some of these optimization methods modify ship hull forms by reducing calm-water drag and wave patterns [10,11]. Campana et al. (2006) optimized the David Taylor Model Basin 5415 using Non-uniform Rational Basis Spline *(NURBS)* surface modeling and Reynolds Average Navier-Stokes (RANS) code to minimize the total resistance [12].

Reduction of the wave resistance can often be obtained without any significant decrease in the amount of displacement volume. The sensitivity of the wave resistance to hull form design modifications and the accuracy of potential flow solver were chosen as the objective function of optimization procedure by Matulja and Dejhalla [13]. The potential flow solver and the genetic algorithm were coupled for bulbous bow optimization. The results showed 10% reduction in wave resistance coefficient at the design speed, corresponding to Froude number of 0.289. The results for a wide range of Froude numbers are shown in Figure 1.
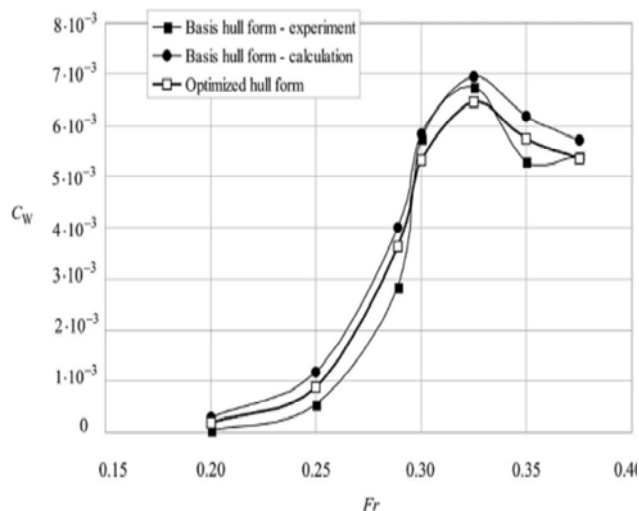
Figure 1. Wave resistance coefficients versus Froude number [13]

It was reported that the maximum reduction in CO_2 emission is about 2-3% by optimal hydrodynamic design [8].

2.1. Modern Hull

In recent years, interests to use high-speed vessels are significantly increasing specially in military, recreational, racing, and transportation applications.

There are several ways to increase the Froude number of a hull. The main way is to rearrange the displacement hulls into segments with shorter lengths, using techniques such as: air cushions, Wing In Ground (WIG) effect, and hydrofoil or a combination of the methods. For the high speed ships, Froude number is approximately greater than 0.4 and wave resistance plays a major role in determining the total resistance. As shown in Figure 2, marine vehicles are divided into two main categories based on the lifting forces acting on them [14].
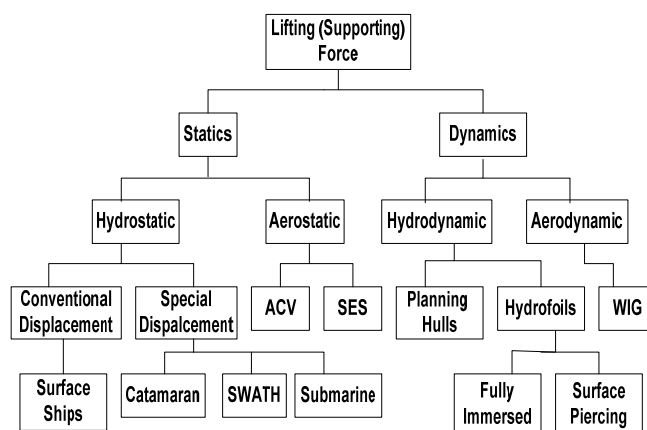
Figure 2. Marine vehicles classification [14]

2.2. Multihull Ships

One approach to have a high speed ship or marine vessel is to decrease the deck area by applying multihulls with very thin water line entrance angles, while ensuring sufficient stability. Multihull vessels owing to their stability and payload capability are

widely employed in military and commercial applications at high operational speeds. To optimize the performance of multihull ships in terms of resistance and seakeeping characteristics, additional efforts are required to perform to characterize their salient hydrodynamics features [15].

2.3. Small Waterplane Area Twin Hull (SWATH) and SLICE

The SWATH is a hull design, which minimizes the waterline level compared to the single-hulls and catamarans; therefore, makes the hydrostatic restoration forces decrease, as illustrated in Figure 3. SWATH water plane area is expressed as a function of the volume displacement and has a direct relationship with wave making resistance and sea-induced ship motions [16].
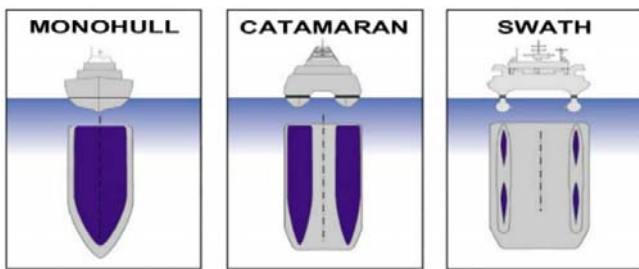
Figure 3. Waterline area of a monohull, catamaran and SWATH [16]

Brizzolara [17] optimized SWATH hull form with an automatic method to achieve the lowest drag at the high speeds. He obtained four optimized underwater hulls at four reference speeds. Examples of corresponding demi-hull panel meshes are given in Figure 4. An underwater hull form with two higher diameters positioned at the bow and stern and a slender diameter in between was considered to this end.
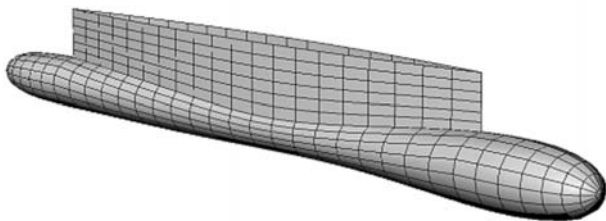
Figure 4. Optimal underwater hull form of SWATH at Froude number of 0.5 [17]

SLICE is a new, patented ship technology that enables SWATH ships to operate at higher speeds while retaining their characteristic low motions in a seaway. SLICE vessel significantly reduces the power consumption at higher speeds. Ability of the SWATH/SLICE vessels to keep track is very high and they have a high transverse oscillation period because of the lower draft [18,19].
Unlike the SWATH, SLICE has four shorter struts and four shorter tear drop-shaped submerged hulls. This structure allows the SLICE hull to reduce wave-making resistance at high speeds for up to 35% compared to a SWATH with the same displacement. In addition, SLICE short hulls are able to push through the wave hump much more quickly. Moreover, SLICE has the same stable ride as a SWATH, but can go faster with the same horsepower, as shown in Figure 5. Furthermore, the comparison of the vessels with the same displacement shows that the length of the SLICE vessels is one quarter of the SWATH hulls length. For the same operational speed, this innovation doubles the Froude number [20].
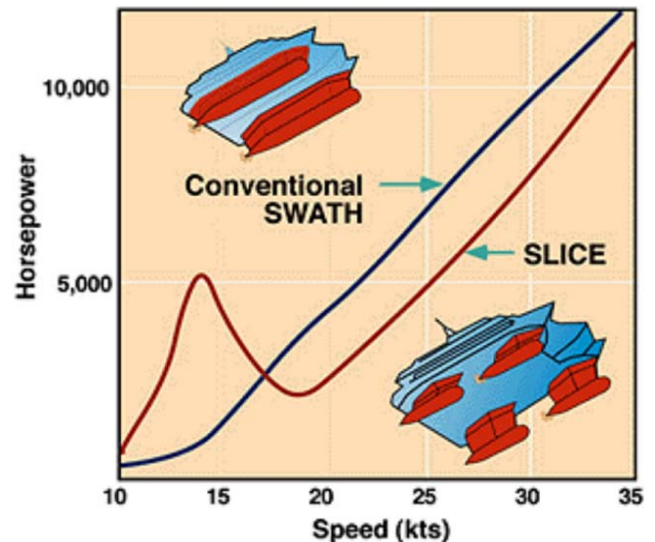
Figure 5. The power requirement of SWATH and SLICE at different speeds [21]

2.4. Air Cushion Vehicles (ACVs)

ACVs are vehicles supported vertically by an air-cushion. In this technology air is supplied from a lift fan, which provides air flow round the periphery of the hull followed by the ejection into the cushion space. Air-cushion may also provide a vehicle with capability to move both on land and sea surfaces [20]. Another type of vessels, which operates like an ACV is commonly known as the surface effect ships (SES). It is a catamaran type vessel, which contains an air cushion between both side hull structure at the forward and the end [22].

2.5. Planing Craft

At low speeds, every hull performs as a displacement hull and as the speed increases, hydrodynamic lift increases as well. When the lift becomes the predominant upward force on the hull, the vessel called to be in the planing mode [23].
A planing hull is a marine vessel, whose weight is mostly supported by the hydrodynamic pressure at the high-speed forward motion. A planing hull speed can be very high; however, it requires more power to get up on top of the water. In addition, a planing hull at low speeds has the worst performance [24]. A typical resistance curve of a planing craft in three modes of motion is shown in Figure 6.
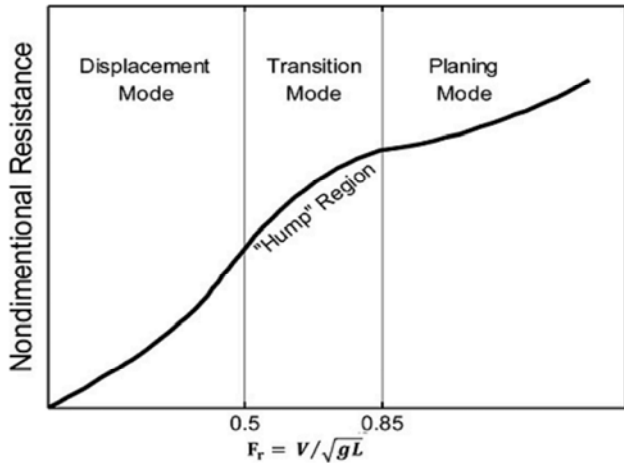
Figure 6. Resistance curve of a planing hull at different modes of motion [24]

2.6. Hybrid Lifting Body Ship

By transferring displacement volume from the parent hull to the lifting bodies, the wetted surface area of the parent hull is reduces, thus reducing its friction drag. The lifting body itself is designed to be a hydro-dynamically efficient shape, with a high lift to drag ratio. The MIDFOIL and HYSWAC are two types of marine vehicles benefit lifting bodies attached under the middle of the vehicle, as shown in Figure 7. Research results reported 15-30% reduction in drag over a wide speed range compared to a conventional mono-hull [25].

(a)   (b)
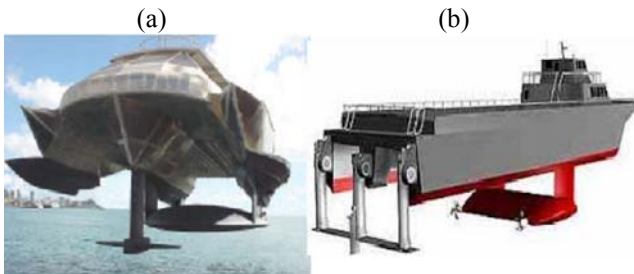
**Figure 7. Hybrid lifting body ships;
(a): MIDFOIL, (b): HYSWAC [26]**

2.7. Wing-In-Ground (WIG) Craft

It has been recognized that flight close to the boundaries (water surface or rigid wall) is more aerodynamically efficient than flight in the free stream flow due to WIG effect. By decreasing the flight altitude, this effect shows the enhancement of lift-to-drag ratio [27].

WIG vehicles fly close to the water surface by utilizing a cushion of relatively high-pressure air between the wings and the water surface [28]. The aircushion augments lift and reduces drag considerably compared to an out-of-ground effect vehicle [29-31].

Despite the low operational expenses of WIG vehicles and their fast movement compared to the aircraft and high speed ships, WIG vehicles are challenged by technical difficulties such as hump drag. Hump drag

impedes the high speed needed to take off. In addition, it causes instability problems, which is not generally observed in a typical airplane [32,33]. Figure 8 shows the hump drag profile of various marine vehicles.
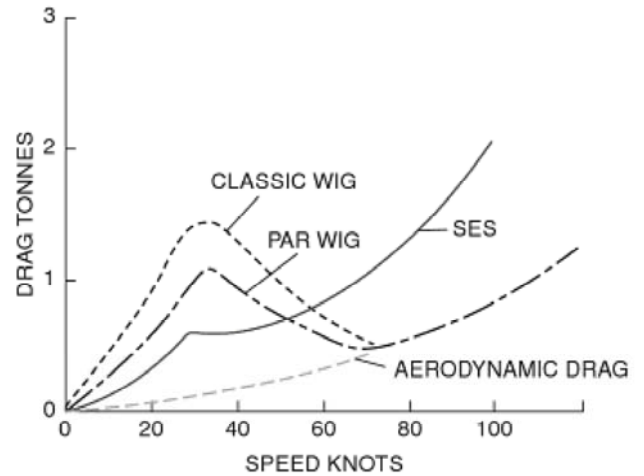
Figure 8. Hump drag at various speeds [33]

3. Air Lubrication

Air lubrication technique is the injection of air around the hull surface, which either creates a bubbly flow or a blanket of gas. In the last decade, there has been a renewed interest in the application of air lubrication in marine vessels and a significant amount of researches have been conducted.

The economic and environmental effects of successfully implemented air lubrication could be significant, as the ship's fuel consumption may be reduced by 5 to 20% [34]. This technique was categorized into three sections namely, Micro-bubble Drag Reduction (MDR), Air Layer Drag Reduction (ALDR), and Partial Cavity Drag Reduction (PCDR).

3.1. Micro Bubble Drag Reduction (MDR)

The first experimental work on MDR method presented by McCormick and Bhattacharya (1973) [35]. Small bubbles were created around a fully submergible hull by using a copper wire wrapped around it. Merkle and Deutsch (1989) showed that micro-bubbles injection became ineffective for low speed conditions due to buoyancy [36]. In addition, it was reported that with increasing the Reynolds number in a micro-bubble-laden turbulent boundary layer, the amount of drag reduction decreases [37]. Therefore, the most influence of bubble injection on drag reduction occurs within a particular speed range. It was reported that by the application of MDR method, up to 80% reduction in the drag could be achieved [38].

Effect of micro-bubbles on turbulent boundary layer and factors affecting the bubbles are two important subjects in bubble injection technique, which will be discussed in the following subsections.

3.1.1. Turbulence Modification with Micro-bubbles

Fluid flow behavior near the solid boundaries is a complicated issue. Absence of analytical solutions, deficiency of empirical researches, and lack of understanding about the mechanism of drag reduction by micro-bubbles has led the lack of an accurate model for this phenomenon. Some researchers believe that the drag reduction by micro-bubbles is the result of thickening the boundary layer due to an increase in the viscosity and a reduction in the density of the buffer layer. Legner (1984) believed that the drag reduction was obtained by the combination of density reduction and turbulence modification [39]. In another report, Kanai and Miyata (2001) explained that the bubbles prevented span-wise eddies formation near the wall, and this led to suppression of turbulence bursting phenomenon and reduction of turbulent energy [40].

The most efficient domain for accumulation of the micro-bubbles in the boundary layer is buffer region, and its due to the fact that by increasing the density of micro-bubbles, turbulence intensity of buffer layer decreases [41,42]. Villafuerte and Hassan (2006) showed that the desirable concentration of micro-bubbles between a y+ range of 15–30 plays a dominant role in effecting the turbulent structure change along the boundary layer [43]. However, it was also shown that the presence of the micro-bubbles can be felt for $y^+ \geq 10$, as illustrated in Figure 9 [44]. According to the Figure 9, although the inner layer approximately does not change, viscous zone has a gradual thickening trend with an upward shift of the logarithmic region during the micro-bubbles injection. In Figure 9, free stream velocity is 14.2 m/s and air flow rates varying from $Q_1=0.001$ m^3/s to $Q_5=0.003$ m^3/s.
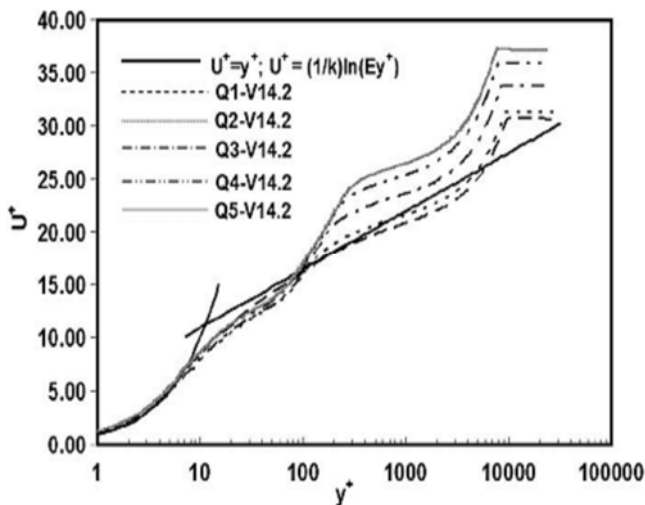
Figure 9. Change in the boundary layer at different gas flow rates [44]

3.1.2. Factors Affecting Bubbles

Numerous laboratory experiments have been reported the effectiveness of using micro-bubbles technique in ships' hull drag reduction. However, there are many ambiguities about the suitability of this technique such as: volume fraction, injection rate, bubble size, best injection method, buoyant force, performance in salt water, and distance from the injection point.

Lu et al. (2005) believes that bubbles' deformability plays an important role in the bubbles drag reduction [45]. It was also shown that the increase in the main flow velocity causes a larger reduction rate for the skin friction. Furthermore, it was also proved that, bubbles with the diameter larger than the scale of boundary layer will make the drag to increase (bubbles with the diameter range of 2-3 mm) [46].

In another study, photographic records showed that mean bubble diameter decreases monotonically with the salinity increase [47].

Density ratio is another parameter, which was studied numerically and it was indicated that at a low gas injection flow rate and density variation between 0.2 and 0.001 has not considerable effect on the drag reduction. However, it was shown that for high gas injection flow rates with decreasing density ratio drag reduction rate gradually increases, as illustrated in Figure 10 [38].

Downstream distance of the injection point, the drag reduction is decreased as a result of bubbles migration from the near-wall region. Air lubrication experiments on a 40m long plate revealed that the effect of micro-bubbles disappears after half-length of the plate [48].
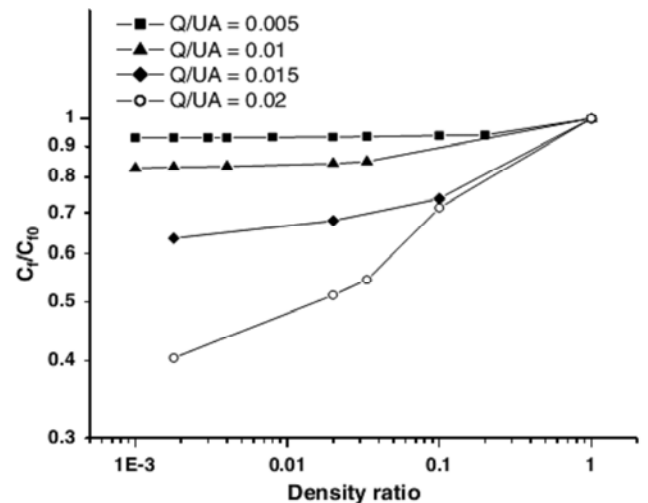
Figure 10. Density ratio effect on the drag reduction [38]

Elbing et al. (2008) applied two different types of injectors and the results of Bubble Drag Reduction (BDR) experiments indicated that a porous-plate injector versus a slot injector is more efficient at higher flow speeds, as shown in Figure 11 [49]. In Figure 11, a comparison of the slot (solid symbols) and porous-plate (open symbols) injectors at the four gas injection rates is presented. It was also shown that drag reduction is lost 2 meters downstream of the injection site and BDR has negligible sensitivity to the surface tension. Moreover, it was shown that BDR is insensitive to the boundary-layer thickness at the

injection location and synergetic effect was not observed with the compound injection.
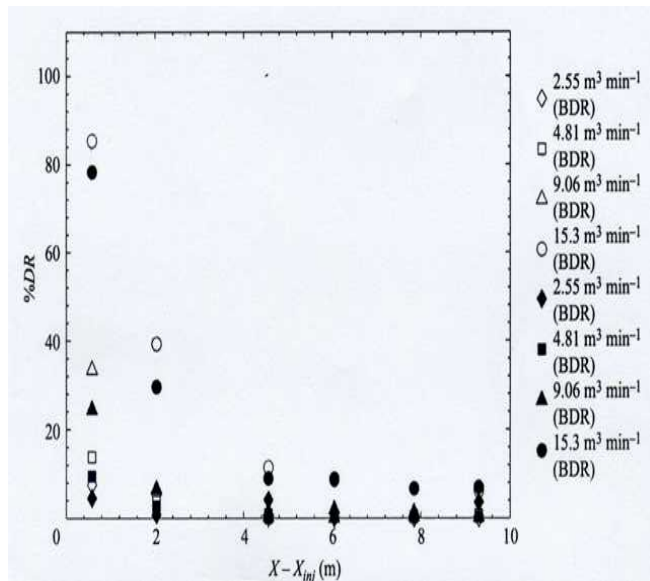
Figure 11. Effect of distance from the injector at a free-stream speed of 20 m/s on Drag Reduction (DR) [49]

3.2. Air Layer Drag Reduction (ALDR)

ALDR method is performed by forming a continuous air layer between the hull and liquid, as illustrated in Figure 12 [34].
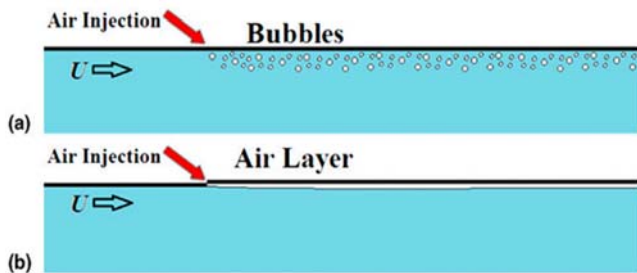
Figure 12. Two types of air lubrication techniques [34]

As Figure 13 indicates, drag reduction with the air injection method can be divided into three distinct regions. First region is BDR zone, where drag reduction grows linearly with gas injection rate. Another region is ALDR, where a maximum level of drag reduction is achieved. A transition area is also located between these two regions, where drag reduction increases linearly with a higher trend than the BDR zone [49].

Elbing et al. (2008) also found that the critical volumetric air flux to achieve ALDR is approximately proportional to the square of the free-stream speed [49]. For a surface fully roughened, nearly 50% higher volumetric air flux is required to form a stable air layers at free-stream speeds up to 12.5m/s. It was also observed that ALDR is sensitive to the inflow conditions.
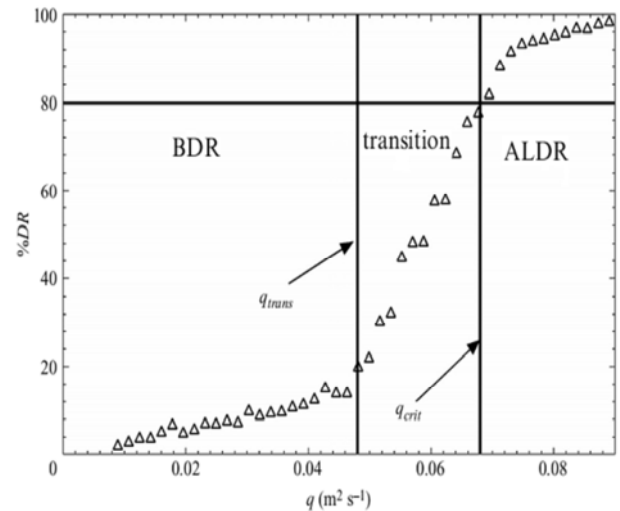
Figure 13. Percentage of Drag Reduction (DR) versus volumetric gas injection rate per unit span (q) [49]

3.3. Partial Cavity Drag Reduction (PCDR)

PCDR method creates a continuous lubricating gas layer like ALDR method. Where the cavity length could not be extended to the whole craft length at low speed conditions, Butuzov et al. (1999) utilized a series of steps to extend the cavity at the whole bottom of the ship. Figure 14 shows two type of air-cavity systems [50].

The primary usage of artificial air cavity was adapted in flying boats [51]. Matveev et al. (2009) studies showed that stability of large area cavities must be maintained at low flow rates for the air injection [52].
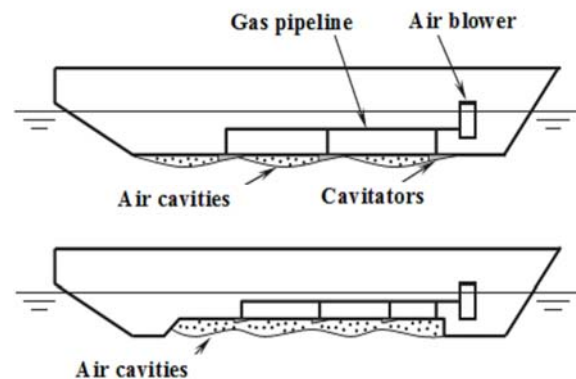
Figure 14. Air-cavity systems and bottom recess applied on displacement vessels [53]

Drag reduction of planing hulls due to the artificial air cavity utilization is 20–35%, while it is 15–30% for semi-planing hull forms. The air supply pressure in the cavity is retained by low pressure air fans, and power consumption due to air flow fans is reported to be within 3% of the main engine power [50,54].

Air cavity ships have several other applications such as: lowering underwater hull noise radiation and shocks and reduce wave drag, especially on multi-hull vessels [55-56].

PCDR method requires more modifications at the bottom of the hull. In addition, the initial investment cost of PCDR is more than ALDR, while its operating

cost is less and potentially offers larger frictional drag reduction with a lesser gas flux (see Figure 15) [34].
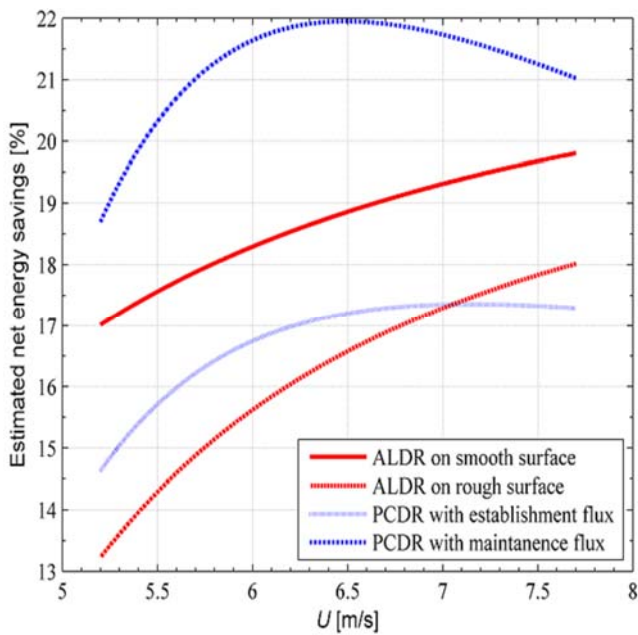
Figure 15. Net energy savings for a ship by using air lubrication technique [34]

4. Fouling and Coating

One of the best methods to reduce frictional resistance is to apply a treatment on the ship hull to minimize its physical and biological roughness. Any increase in the underwater hull roughness will make a significant rise in vessel operating costs.

Hull roughness is considered as the skin friction and depends on the type of coating, amount of rust, fractures in the coating, and fouling. Physical roughness can be minimized by applying some preventative measures; however, it is very difficult to control the biological roughness (fouling) [57]. Figures 16 and 17 show the physical and biological roughness, respectively.
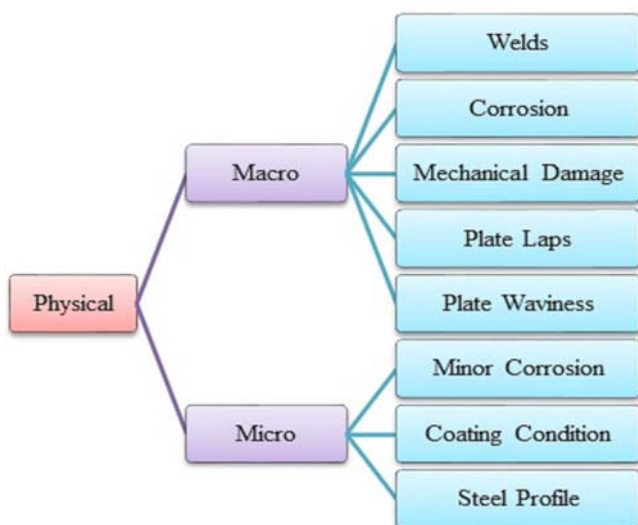
Figure 16. Physical roughness [57]
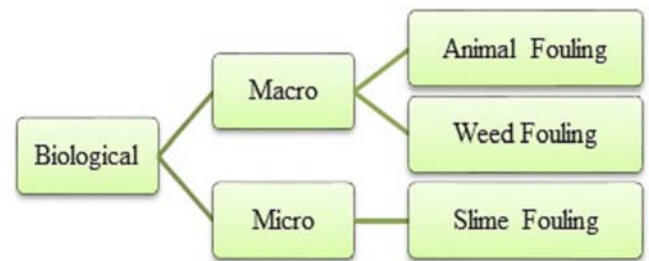
Figure 17. Biological roughness [57]

4.1. Roughness Allowance

Hull roughness resistance normally increases during the ship life time owing to marine fouling. The naval architecture community includes the effects of surface roughness in an allowance coefficient, which is added to the smooth surface friction and residual resistance coefficients when determining the overall drag of a full scale ship [58].

Bowden-Davison (1974) recommended a formula as a function of the mean hull roughness and was intended to be used as an allowance coefficient by International Towing Tank Committee to predict the ship resistance. However, the recommended relationship is not an accurate hull roughness penalty predictor, since it includes additional residual components of resistance prediction, including model scale effects [59].

Friction coefficient due to roughness is not independent of Reynolds number, since ships do not necessarily operate in the 'fully rough' region, and Townsin et al. (1984) provided a formula for predicting the roughness penalty based on the mean hull roughness and the Reynolds number [60].

4.2. Roughness and Fouling

When the boundary layer is thin, the roughness effect is significant. It also has a considerable effect, where the local flow speed is high. Therefore, roughness effects near the stern are less than the bow and at the bilge are more than the waterline. Roughness only increases the drag if it is large enough to project through the sublayer. As Reynolds number increases, the sublayer gets thinner and eventually drag coefficient becomes approximately constant (see Figure 18) [58].

In recent decades, numerous researches have been conducted to study the roughness effects on Ships' performance such as experiments on flat plates or ship hulls. For instance, Yokoi [62] examined the shaft horse power and fuel consumption of a training ship over eight years to estimate the effect of bottom fouling. The results showed that the shaft horse power increases about 20% in full speed condition. Doi and Kikuchi [63], explored the frictional resistance coefficient of five coarsen plates from an actual ship hull under a circulating water channel. The results showed the speed decrease of 0.1-1 m/s and

0.15-1.54 m/s for the blunt ships and high speed ships, respectively due to roughness.
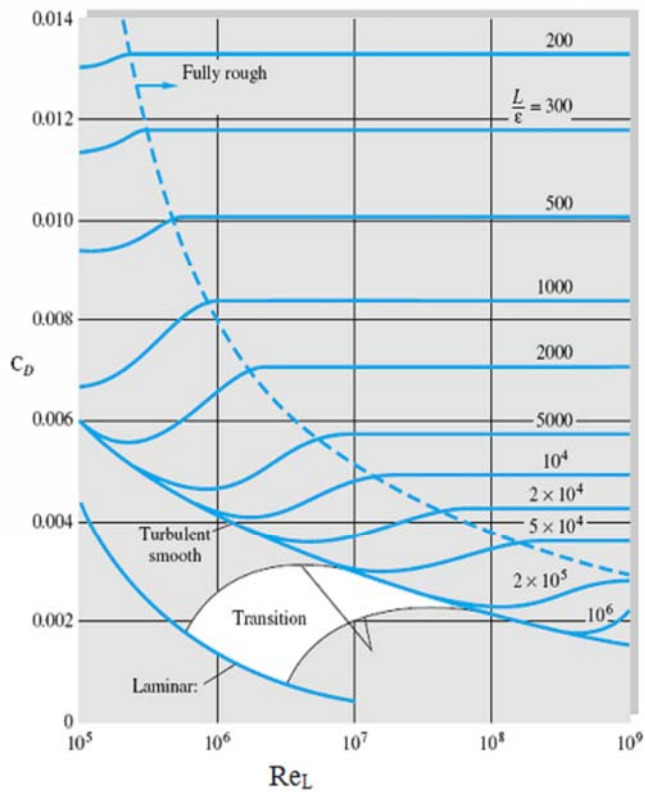
Figure 18. Resistance diagram for rough plate with sand roughness [58]

While the roughness parameter is still only based on roughness height measurements and other characteristics of the roughness does not account, International Towing Tank Conference (ITTC) report indicated that the methods used to rectify the hull roughness and fouling have uncertain accuracy [64]. In another study, Schultz [65] compared the resistance of a ship model with boundary layer similarity law analysis in some roughness conditions. The study proved that in heavy calcareous fouling the total resistance increases up to 80%.

4.3. Marine Fouling

Marine bio-fouling can be defined as the undesirable accumulation of organisms and biogenic structures on the ship hulls and other submerged surfaces [66]. Bio-foulings, can be divided into two different categories in term of coarseness namely, micro-fouling (bacteria and diatomic biofilms) and macro-fouling (macro algae, barnacles, bryozoans, mussels, and tube worms). These living organisms immediately attach to the immersed surfaces and grow until several months after immersion [67].

Slime or algae is an example of micro-fouling organisms and raise the resistance for about 1-2%. Hard-shelled fouling species such as barnacles, tube worms, and mussels may increase ship resistance up to 40%. Figure 19 shows the different fouling types on the ship's hulls [68].

(a) (b) (c)
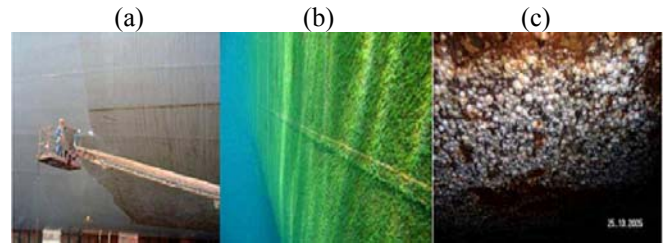
Figure 19. Three types of marine fouling;
(a): Slime, (b): Weed, (c): Hard [68]

Ability of marine fouling to settle and grow depends on the factors such as: salinity, pressure, and nutrient levels. In addition, the physical properties of the surface such as: roughness, color, and surface wettability can affect both biofilm composition and larval settlement [69].

Schultz and Swain [70] compared turbulent boundary layers over the natural marine biofilms and a smooth plate. The study showed an average increase of 33%-187% for the skin friction coefficient by measuring the velocity components profiles. It was also found that the skin friction coefficient depends on biofilm thickness and surface shape.

For the global shipping industry, bio-fouling costs billions of dollars per a year to prevent and maintenance.

4.4. Antifouling Coating

Another method to prevent the increase of skin friction is smoothing the surface through the use of antifouling coatings; however, these coatings offer no improvement over a clean smooth hull surfaces. One of the well-known surface coating is antifouling paints, which applied to the hulls of boats and static submerge structures. Antifouling paints prevent the growth of fouling organisms by releasing biocides.

Ships hull roughness due to the fouling and coating defects increase the turbulent and wall shear stress in the boundary layer; therefore, directly increases power requirements [71].

For a mid-size merchant and naval vessel at cruising speed, about 21% of propulsive power is consumed to overcome the increases in resistance and powering due to slime films and up to 86% is consumed due to heavy calcareous fouling [65].

With the phasing out and ultimate ban on triorganotin (tributyltin), new alternatives have been developed to apply as the antifouling coating. Tin-free self-polishing coatings, silicone-based foul release coatings, hydrophilic marine antifouling coatings and hydrophobic foul-release coatings are some nontoxic alternatives recommended for this purpose[72-75].

Schultz [76] measured frictional resistance and velocity distribution on the surfaces coated with silicone, ablative copper, tributyltin self-polishing copolymer (TBT SPC) and SPC copper in the fouled, unfouled, and cleaned conditions. After 287 days of marine exposure, experimental results indicated that the largest increases in the frictional resistance

coefficient belongs to a surface coated with silicone. In another research study, Willsher [68] compared the effect of biocide free foul release coating with biocidal antifouling and concluded that both hull roughness and environmental impact of foul release against its initial costs is lower than biocidal antifouling.

Foul release systems work quite differently and they inherently rely on an ultra-smooth surface by providing a low-friction surface to minimize the adhesion of fouling organisms. Because of weak bonding between the fouling and the foul release coating surface, fouling can be easily removed either by an underwater cleaning or by a hydrodynamic force.

Figure 20 shows the total resistance coefficient for two different antifouling coating over at the speed range of 2 - 8 m/s. Based on the result, the surface coated with a foul release system shows lower drag [77]. In addition, it was found that foul release coatings reduce frictional resistance 2–5% more than self-polishing coating [75].
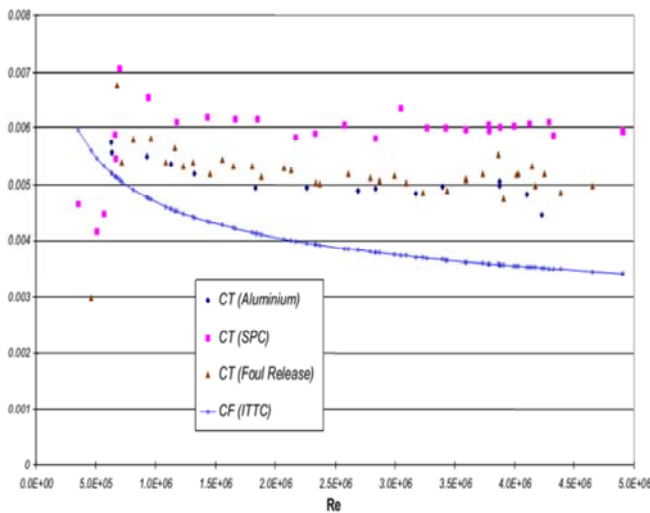
Figure 20. Total resistance coefficients against Reynolds number for the three tested surfaces [77]

4.4.1. Surface Energy

The molecules on the surface have more energy compared with the molecules in the bulk of the material. Therefore surface energy is excess energy at the surface of a material compared to the molecules in the thermodynamically-homogeneous interior. The surface energy shows the ability of a surface to interact with other materials [78,79]. Baier [80] studies showed that there is a direct relationship between the surface energy and the adhesion of fouling. It is found from Figure 21 that by reducing the surface energy in a certain range, the adhesion strength of biological fouling are minimized.

In addition to the surface energy, elastic modulus, thickness, and smoothness are very important factors for an effective foul release coating. Surface roughness increases the surface area available for

attachment of fouling and also protects fouling from shear and abrasion (hydro-dynamical removal) with situating in the valleys of rough surfaces [77].
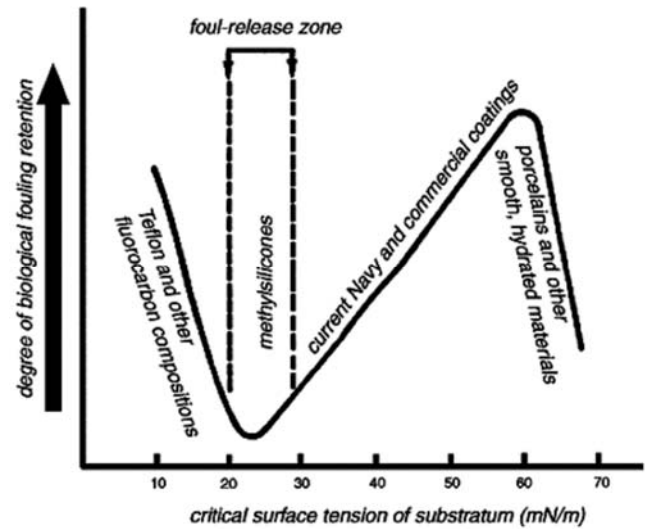
Figure 21. Critical surface tension for minimizing fouling adhesion [81]

4.5. Super-hydrophobic Surfaces and Riblets

The leaves of the lotus plant in Figure 22 are known to be super-hydrophobic and self-cleaning because of their unique surface structure [82]. Hydrophobic structures are capable of staying dry under water for several days by trapping a layer of air [83]. When the percentage of air pores in a super-hydrophobic surface is sufficiently high, slip effect can cause the skin-friction reduction [84].
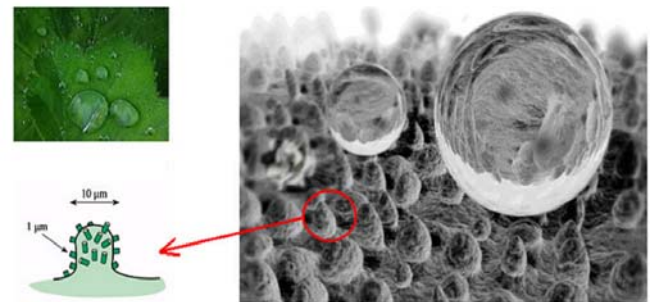
Figure 22. Lotus leaf's super-hydrophobicity and its multi-scale topographic surface [85]

The air layer on a super-hydrophobic surface underwater is unsteady, which might even disappear, depending on the amount of hydraulic pressure applied on the surface. Keeping the hydraulic pressure below the critical pressure may be necessary to realize the low drag or friction reduction applications of the super-hydrophobic surface underwater [86].

The main reasons of the surface hydrophobicity characteristics failure in the turbulent flow regime are lack of robust air on the hydrophobic surface and failure of the nano or micro textures. One way to satisfy these requirements is the application of super-hydrophobic hyper-branched polymer coatings with hierarchic nano/micro textures. If super-hydrophobic

technology for drag reduction is successful, the technology would greatly reduce the cost of the fuel for marine vessels and will increase the speed of them [87].

In a turbulent-flow regime, drag reduction can occur when the flow direction is parallel to the micro ridges structure, while spanwise ridges could make the drag to increase [88]. Hydrophobicity reduces the ability of any fouling organism larger than a bacterium to adhere to the vessel; therefore, shear stress at the surface can easily dislodge any bonded fouling [89]. The super non-stick properties of the super-hydrophobic surfaces will provide an even better ability to prevent the accumulation of marine organisms on ships' hulls compared to the silicone-based coatings [87]. These features are considered to make artificial nano engineered super-hydrophobic surfaces applied to reduce marine fouling resistance [90]. Samples of artificial nano engineered surfaces are shown in Figure 23. By super imposing a nano-structure into a micro fabricated structure, the slip length can be maximized, and thus the rate of drag decline will be increased [91].

Micro-fabrication method could be utilized to produce super-hydrophobic surfaces with different properties. However, production cost is probably the most prohibitive issue for commercializing micro-fabricated surfaces. In addition, it cannot be applied to large-scale bodies with arbitrary shapes too.
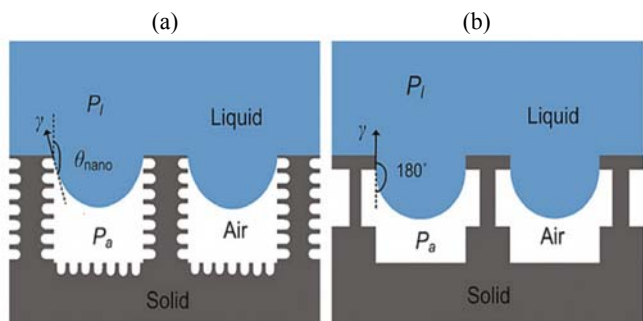
Figure 23. Nano engineered super-hydrophobic surfaces; (a): Nanostructures on the sidewall, (b): Re-entrant structure [91]

It was shown that wall surfaces with micro-grooves, so-called riblets, in turbulent boundary layers lead to a net drag reduction for about 10%. Riblets are streamwise microgrooves, which act as a fence against the break up spanwise vortices, and consequently reduces the surface shear stress and momentum losses [92,93]. The development of riblets to reduce turbulent skin friction came in part from the study of shark scales. Riblets are believed to lift and pin the naturally occurring fluid vortices in the viscous sublayer. Lower drag increases fluid flow at the skin, reduces microorganism settlement time, promotes washing, and allows for faster swimming [94-98] (see Figure 24).
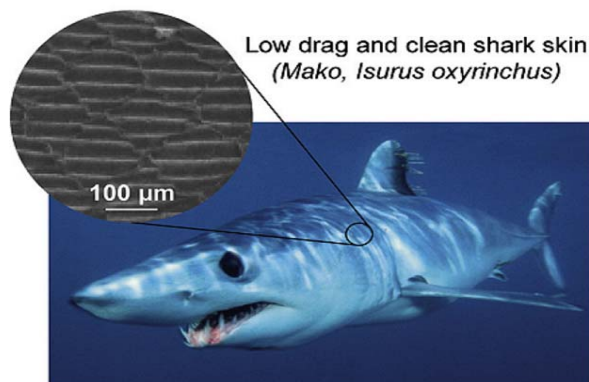
Figure 24. Mako shark skin microstructure riblets [99]

5. Conclusions

In the present paper, a literature review was carried out on the methods implemented for reducing ship hull resistance to improve the hydrodynamic performance. The methods were categorized into three main sections, which focused in turn on the hull forms and its optimization, air lubrication, and fouling and coatings. For every category, the conducted experimental and theoretical studies were reviewed and the key benefits of the various technologies highlighted.

The literature survey revealed that to improve the hydrodynamic performance of the marine vessels, frictional and pressure resistance need to be decreased. It was found that the practical optimization of ship hull form due to the complexity and its time-consuming process is done mostly by large ship building industry. It was also shown that ship hull form optimization reduces only a small percentage of the total ship resistance. Moreover, it was shown that the design and optimization of new hull forms lead to a significant reduction in drag. For this reason, the application of this type of vessels has been expanded in various fields nowadays.

Literature review showed that the air lubrication method has desired effect on ship hull drag reduction by reducing the bubbles diameter and density ratio, or increasing the boundary layer thickness, gas flow rate and main flow velocity, and since many aspects of the behavior of air in water are poorly understood, air lubrication techniques can effectively increase the resistance of a ship hull. In addition, it was found that many other factors are effective in the air lubrication drag reduction method and it requires further research in the field. Moreover, the review indicated that the best way to prevent an increase in frictional drag caused by fouling is to use antifouling coatings and foul release coatings. Among these, foul release systems work quite differently and they inherently rely on an ultra-smooth surface by providing a low-friction surface to minimize the adhesion of fouling organisms.

Based on this literature survey, the most direct way of minimizing the drag forces can be achieved by effective hull form optimization methods combined

with advanced hull drag reduction techniques. New methods for drag reduction are still being investigated and considerable studies are required for their application in marine transportation.

6. Acknowledgment

7. References

1- Royal Academy of Engineering, (2013), *Future Ship Powering Option*, available at: https:/www.raeng.org.uk.

2- IMO, (2009), *Second IMO GHG Study*, Marine Environment Protection Committee.

3- Li, P.Y., Qiu, Y.M. and Gu, M.T., (2002), *Study of trimaran wave making resistance with numerical calculation and experiments*, Journal of Hydrodynamics, Vol. 14(2), p. 99-105.

4- Tarafder, S., (2007), *Third order contribution to the wave making resistance of a ship at finite depth of water*, Ocean Engineering, Vol. 34(1), p. 32-44.

5- Truong, V.T., (2001), *Drag Reduction Technologies, Maritime Platform Division*, Aeronautical and Maritime Research Laboratory, DSTO-GD-0290.

6- Biliotti, I., Brizzolara, S., Viviani, M., Vernengo, G., Ruscelli, D., Galliussi, M., Guadalupi, D. and Manfredini, A., (2011), *Automatic Parametric Hull form Optimization of Fast Naval Vessels*, 11th International Conference on Fast Sea Transportation, Honolulu, Hawaii, USA.

7- Gammon, M.A., (2011), *Optimization of fishing vessels using a multi-objective genetic algorithm*, Ocean Engineering, Vol. 38(10), p. 1054-1064.

8- Han, S., Lee, Y.S. and Choi, Y.B., (2012), *Hydrodynamic hull form optimization using parametric models*, Journal of Marine Science and Technology, Vol. 17(1), p. 1-17.

9- Matulja, D. and Dejhalla, R., (2013), *Optimization of the ship hull hydrodynamic characteristics in calm water*, Shipbuilding, Vol. 64 (4), p. 426-436.

10- Hochkirch, K. and Fassardi, C., (2007), *Analysis of Wave Making Resistance and Optimization of Canting Keel Bulbs*, The 18th Chesapeake Sailing Yacht Symposium, Annapolis, USA.

11- Percival, S., Hendrix, D. and Noblesse, F., (2001), *Hydrodynamic optimization of ship hull forms*, Applied Ocean Research, Vol. 23, p. 337–355.

12- Campana, E.F, Peri, D, Tahara, Y. and Stern, F., (2006), *Shape optimization in ship hydrodynamics using computational fluid dynamics*, Computer Methods in Applied Mechanics and Engineering, Vol. 196, p. 634–651.

13- Matulja, D. and Dejhalla, R., (2012), *Hydrodynamic Optimization of the Fore Part of the Ship*, XX Symposium SORTA.

14- Kotb, M.A. and Rashwan, A.M., (2003), *WIG configuration prediction using neural network approach*, Alexandria Engineering Journal, Vol. 42 (1), p. 9-15.

15- Faltinsen, O., (2005), *Hydrodynamics of High Speed Marine Vehicles*, Cambridge University Press.

16- Grannemann, F., *SWATH – A proven and Innovative Hull Concept*, Abeking & Rasmussen Schiffs- und Yachtwerft Aktiengesellschaft, Mexico.

17- Brizzolara, S., (2004), *Parametric Optimization of SWAT-Hull Forms by a Viscous-Inviscid Free Surface Method Driven by a Differential Evolution Algorithm*, Proceeding of 25th Naval Hydrodynamic Symposium, Saint John's, Canada.

18- Collins, C.A., Clynch, J.R. and Rago, T.A., (2005), *Comparison of SWATH and Monohull Vessel Motion for Regional Class Research Vessels*, Naval Postgraduate School, California, USA.

19- Al-jowder, J.A., (1995), *Comparative Resistance Calculations for SWATH/SLICE Hulls*, Thesis, Naval Postgraduate School, California.

20- Kaya, K., Özcan, O., (2013), *A numerical investigation on aerodynamic characteristics of an air-cushion vehicle*, Journal of Wind Engineering and Industrial Aerodynamics, Vol. 120, p. 70–80.

21- Jansson, B.O. and Lamb, G.R., (1992), *Buoyantly supported multihull vessels, High-Performance Marine Vehicles* Conference, Arlington, MH1-17.

22- Seif, M.S. and Tavakoli, M.T., (2004), *New Technologies for Reducing Fuel Consumption in Marine Vehicles*, XVI Symposium SORTA.

23- Sponberg, E.W., (2011), The Design Ratios, Sponberg Yacht Design Inc,

24- Marshall, R., (2002), *All about power boats: understanding design and performance*, McGraw-Hill Professional.

25- Kona, K., (2006), *The CEROS Newsletter is published by the National Defense Center of Excellence for Research in Ocean Sciences (CEROS)*, Volume 9 (1 & 2), Hawaii 96740.

26- Todd, J. and Peltzer, P.E., (2003), *Lifting Body Technology for Transformational Ship Designs*, 9th Naval Platform Technology Seminar.

27- Rozhdestvensky, K.V., (2000), *Aerodynamics of a lifting system in extreme ground effect*, 1st ed. Heidelberg, Springer.

28- Fach, K., Fischer, H., Kornev, N. and Petersen, U., (2004), W*ing in ground (WIG) effect craft, Chapter 48 in: Ship Design and Construction*, The Society of Naval Architects and Marine Engineers (SNAME).

29- Joh, C.Y. and Kim, Y.J., (2004), *Computational aerodynamic analysis of airfoils for WIG (airfoil-in-ground-effect)-craft*, Journal of the Korean Society for Aeronautical & Space Sciences, Vol. 32 (8), p. 37-46.

30- Rozhdestvensky, K.V., (2006), *Wing-in-ground effect vehicles*, Progress in Aerospace Sciences, Vol. 42, p. 211–283.

31- Kikuchi, K., Motoe, F. and Yanagizawa, M., (1997), *Numerical simulation of the ground effect using the boundary element method*, International Journal of Numerical Methods in Fluids, Vol. 25, p. 1043-1056.

32- Lee, S.H. and Lee J., (2013), *Aerodynamic analysis and multi-objective optimization of wings in ground effect*, Ocean Engineering, Vol. 68, p. 1–13.

33- Yun, L., Bliault, A. and Doo, J., (2010), *WIG craft and ekranoplan: ground effect craft technology*, Springer.

34- Ceccio, S.L., Mäkiharju, S.A., (2012), *Air Lubrication Drag reduction on Great Lakes Ships*, Great Lakes Maritime Research Institute.

35- McCormick, M.E. and Bhattacharya, R., (1973), *Drag reduction of a submersible hull by electrolysis*, Naval Engineering Journal, Vol. 85, p. 11– 16.

36- Merkle, C.L. and Deutsch, S., (1989), *Microbubble Drag Reduction.* Frontiers in Experimental Fluid Mechanics, Vol. 46, p. 291-335

37- Ferrante, A. and Elghobashi, S., (2004), *On the physical mechanisms of drag reduction in a spatially developing turbulent boundary layer laden with microbubbles*, Journal of Fluid Mechanics, Vol. 503, p. 345–355.

38- Skudarnov, P.V. and Lin, C.X., (2006), *Drag reduction by gas injection into turbulent boundary layer: Density ratio effect*, International Journal of Heat and Fluid Flow, Vol. 27, p. 436–444.

39- Legner, H.H., (1984), *A simple model for gas bubble drag reduction*, Physics of Fluids, Vol. 27 (12), p. 2788–2790.

40- Kanai, A. and Miyata, H., (2001), *Direct numerical simulation of wall turbulent flows with micro-bubbles*, International Journal for Numerical Methods in Fluids, Vol. 35 (5), p. 593–615.

41- Madavan, N.K., Merkle, C.L. and Deutsch, S., (1985), *Numerical investigations into the mechanisms of micro-bubble drag reduction*, Journal of Fluids Engineering, Vol. 107, p. 370-377.

42- Kato, H., Iwashina, T., Miyanaga, M. and Yamaguchi, H., (1999), *Effect of micro-bubbles on the structure of turbulence in a turbulent boundary layer*, Journal of Marine Science and Technology, Vo. 4, p. 155-162.

43- Villafuerte, J.O. and Hassan, Y.A., (2006), *Investigation of micro-bubble boundary layer using particle tracking velocimetry*, Journal of Fluids Engineering, Vol. 129, p. 66–79.

44- Mohanarangam, K., Cheung, S.C.P., Tu, J.Y. and Chen, L., (2009), *Numerical simulation of micro-bubble drag reduction using population balance model*, Ocean Engineering, Vol. 36, p. 863-872.

45- Lu, J., Fernández, A. and Tryggvason, G., (2005), *The effect of bubbles on the wall drag in a turbulent channel flow*, Physics of Fluids, Vol. 17, p. 1–12.

46- Kato, H., Miura, K., Yamaguchi, H. and Miyanaga, M., (1998), *Experimental study on micro-bubble ejection method for frictional drag reduction*, Journal of Marine Science and Technology, Vol. 3, p. 122-129.

47- Winkel, E.S., Ceccio, S.L., Dowling, D.R. and Perlin, M., (2004), *Bubble size distributions produced by wall-injection of air into flowing freshwater, saltwater, and surfactant solutions*, Experiments in Fluids, Vol. (37), p. 802–810.

48- Watanabe, O., Masuko, M. and Shirose, Y., (1998), *Measurements of drag reduction by micro-bubbles using very long ship models*, Journal of the Society of Naval Architests of Japan, Vol. 183, p. 53-63.

49- Elbing, B.R., Winkel, E.S., Lay, K.a, Ceccio, S.L., Dowling, D.R. and Perlin, M., (2008), *Bubble-induced skin-friction drag reduction and the abrupt transition to air-layer drag reduction*, Journal of Fluid Mechanics, Vol. 612, p. 201–236.

50- Butuzov, A., Sverchkov, A., Poustoshny, A. and Chalov, S., (1999), *State of art in investigations and development for the ship on the air cavities*, International Workshop on Ship Hydrodynamics (IWSH'99) China, p. 1–14.

51- Bell, J.W., (1935), *The effect of depth of step on the water performance of a flying-boat hull model*, NACA Model 11-0, NACA Technical Notes 535.

52- Matveev, K.I., Burnett, T.J. and Ockfen, A.E., (2009), *Study of air-ventilated cavity under model hull on water surface*, Ocean Engineering, Vol. 36, p. 930–940

53- Matveev, K.I., (2007), *Three-dimensional wave patterns in long air cavities on a horizontal plane*, Ocean Engineering, Vol. 34 (13), p. 1882–1891.

54- Butuzov, A., Sverchkov, A., Poustoshny, A. and Chalov, S., (1999b), *High speed ships on the cavity: scientific base, design peculiarities and perspectives for the Mediterranean sea*, Fifth Symposium on High Speed Marine Vehicles, HSMV'99, Capri, Italy.

55- Matveev, K.I., (2005b), *Effect of drag-reducing air lubrication on underwater noise radiation from ship hulls*, Journal of Vibration and Acoustics, Vol. 127 (4), p. 420–422.

56- Matveev, K.I., Duncan, R. and Winkler, J., (2006), *Acoustic, dynamic and hydrodynamic aspects of air-lubricated hulls*, Proceedings of Undersea Defense Technology Conference, San Diego, CA.

57- IMC., (2004), *Hull Roughness Penalty Calculator*, Available at: http://www.international-marine.com/Literature/ HRPC_Folder_Paper.pdf.

58- Molland, A.F., Turnock, S.R. and Hudson, D.A., (2011), *Ship resistance and propulsion: practical estimation of ship propulsive power*, Cambridge University Press, England.

59- Bowden, B.S. and Davison, N.J., (1974), *Resistance Increments Due to Hull Roughness Associated With Form Factor Extrapolation Methods*, National Physical Laboratory (NPL) Ship Technical Manual 3800.

60- Townsin, R.L. Medhurst, J.S., Hamlin, N.A. and Sedat, B.S. (1984), *Progress in Calculating the Resistance of Ships with Homogeneous or Distributed Roughness*, NECIES Centenary Conference on Marine Propulsion.

61- White, F. M. (1998). *Fluid Mechanics*, McGraw-Hill Higher Education

62- Yokoi, K. (2004), *On the Influence of Ship's Bottom Fouling upon Speed Performance*, Toyama National College of Maritime Technology, Bulletin of Toyama National College of Maritime Technology in Japan.

63- Doi, H. and Kikuchi, O., (1984), *Frictional resistance due to surface roughness (1st Report) - effect on reducing of ship's speed by roughness models*, Journal of the Kansai Society of Naval Architects, Japan, No.194,

64- International Towing Tank Conference ITTC, (2005), *Report of the Powering Performance Committee*, 24th ITTC, Edinburgh, Scotland, UK

65- Schultz, M.P., (2007), *Effects of coating roughness and biofouling on ship resistance and powering*, Biofouling, Vol. 23 (5), p.331-341

66- Scheer, B.T., (1945), *the development of marine fouling communities,* Biological Bulletin, Vol. 89, p. 103–112.

67- Oram, R., (2015), *Balmoral CuNiClad™ marine antifouling system,* Balmoral Offshore Engineering.

68- Willsher J. (2001), *The Effect of Biocide Free Foul Release Systems on Vessel Performance*, Ship Effficency, 1st International Conference, Hamburg, October 8-9,

69- Soliev, A.B., Hoskawa, K. and Enomoto, K., (2011), *Bioactive Pigments from Marine Bacteria: Applications and Physiological Roles*, Evidence-based Complementary and Alternative Medicine : ECAM, Vol. 2011**,** 670349

70- Schultz, M.P. and Swain, G.W., (1999), *The Effect of biofilms on turbulent boundary layers*, Journal of Fluids Engineering, Vol. 121 (1), p. 44-51.

71- Hellio, C. and Yebra, D., (2009), *Advances in marine antifouling coatings and technologies*, Woodhead Publishing Ltd, p. 148–176.

72- Almeida, E., Diamantino, T.C. and De Sousa, O., (2007), *Marine paints: the particular case of antifouling paints*, Progress in Organic Coatings, Vol. 59, p. 2–20.

73- Chambers, L.D., Stokes, K.R., Walsh, F.C. and Wood, R.J.K., (2006), *Modern approaches to marine antifouling coatings*, Surface and Coatings Technology, Vol. 201, p. 3642–3652.

74- Buskens, P., Wouters, M., Rentrop, C. and Vroon, Z., (2013) , *A brief review of environmentally benign antifouling and foul-release coatings for marine applications,* Journal of Coatings Technology and Research, Vol. 10 (1), p. 29-36.

75- Candries, M. and Atlar, M. (2003), *On the drag and roughness characteristics of anti-foulings,* Transactions of the Royal Institution of Naval Architects, Vol. 145, p. 107–132.

76- Schultz M.P., (2004), *Frictional resistance of antifouling coating systems*, Journal of Fluids Engineering, Vol. 126 (6), p. 1039-1047.

77- Candries, M., Atlar, M. and Anderson, C.D., (2001), *Foul Release systems and drag, Consolidation of Technical Advances in the Protective and Marine Coatings Industry*, Proceedings of the PCE Conference, Antwerp.

78- Brady, RF Jr, Singer, I.L. (2000), *Mechanical factors favoring release from fouling release coatings*, Biofouling, Vol.15, p. 73–81.

79- Vincent, H.L. and Bausch, G.G., (1997), Silicon fouling release coatings, Naval Research Reviews, Vol. 49, p.39–45.

80- Baier, R.E., (1973), *Influence of the initial surface condition of materials on bioadhesion*, Proceedings of the Third International Congress on Marine Corrosion and Fouling, Northwestern University Press, Evanston, p. 633–639.

81- Ciriminna, R., Bright, F.V. and Pagliaro, M., (2015), *Ecofriendly Antifouling Marine Coatings*, American Chemical Society Sustainable Chemistry and Engineering, Vol. 3, p. 559-565.

82- Cheng, Y.T., (2006), *Effects of micro- and nano-structures on the self-cleaning behavior of lotus leaves*, Nanotechnology, Vol. 17, p. 1359–1362.

83- Koch, K., Bhushan, B. and Barthlott, W., (2009), *Multifunctional surface structures of plants: an inspiration for biomimetics*, Progress in Materials Science, Vol. 54, p. 137–178.

84- Rothstein, J.P., (2010), *Slip on super hydrophobic surfaces*, Annual Review of Fluid Mechanics, Vol. 42, p. 89–109.

85- Cui, J., Li, W. and Lam, W.H., (2011), *Numerical investigation on drag reduction with superhydrophobic surfaces by lattice-Boltzmann method*, Computers and Mathematics with Applications, Vol. 61**,** p. 3678-3689.

86- Sheng, X. and Zhang, J., (2011), *Air layer on super hydrophobic surface underwater*, Colloids and Surfaces A: Physicochemal and Engineering Aspects, Vol. 377 (1-3), p. 374–378.

87- Hu, J., (2006), *Skin-Friction Drag Reduction from Super hydrophobic Coatings of Textured Hyper branched Polymers,* Navy STTR FY2006, available at: http://www.navysbir.com.

88- Woolford, B., Prince, J., Maynes, D. and Webb, B.W., (2009), *Particle image velocimetry char-acterization of turbulent channel flow with rib patterned super hydrophobic walls*, Physics of Fluids, Vol. 21.

89- Salta, M., Wharton, J. A., Stoodley, P., Dennington, S.P., Goodes, L.R., Werwinski, S., Mart, U., Wood, R.J. and Stokes, K.R., (2010), *Designing biomimetic antifouling surfaces*. Philosophical Transaction A Math Physics Engineering Science, Vol. 368**,** p. 4729-4754.

90- Scardino, A.J., Zhang, H., Cookson, D.J., Lamb, R.N. and De Nys, R., (2009b), *The role of nano-roughness in antifouling*, Biofouling, Vol. 25, p. 757–767.

91- Lee, C. and Kim, C.J., (2009), *Maximizing the giant slip on super hydrophobic microstructures by nanostructuring their sidewalls*, Langmuir, Vol. 25, p. 12812–12818.

92- Bechert, D.W. Bruse, M., Hage, W., Van der Hoeven, J.G.T. and Hoppe, G., (1997), *Experiments on drag-reducing surfaces and their optimization with an adjustable geometry*, Journal of Fluid Mechanics, Vol. 338, p.59–87.

93- Walsh, M.J. and Weinstein, L.M., (1979), *Drag and heat-transfer characteristics of small longitudinal ribbed surfaces,* AIAA Journal, Vol. 17(7), p. 770-771.

94- Lee, S.J. and Lee, S.H., (2001), *Flow field analysis of a turbulent boundary layer over a riblet surface*, Experiments in Fluids, Vol. 30, p. 153-166.

95- Krieger, K., (2004), *Do pool sharks really swim faster?* Science, Vol. 305, p. 636–637.

96- Dean, B. and Bhushan, B. (2010), *Shark-skin surfaces for fluid-drag reduction in turbulent flow: a review*, Philosophical Transactions of the Royal Society, Vol. 368, p. 4775-4806.

97- Deyuan, Z., Yuehao, L., Xiang, L. and Huawei, C., (2011), *Numerical simulation and experimental study of drag-reducing surface of a real shark skin*, Journal of Hydrodynamics, Vol. 23, p. 204-211.

98- Oeffner, J. and Lauder, G.V., (2012), *The hydrodynamic function of shark skin and two biomimetic applications*, Journal of Experimental Biology, Vol. 215, p. 785-795.

99- Bixler, G.D. and Bhushan, B., (2013), *Fluid drag reduction with shark-skin riblet inspired microstructured surfaces*, Advanced Functional Materials, Vol. 23, p. 4507-4528.